Contribution from the Laboratoire de Chimie de Coordination du CNRS,† 205 route de Narbonne, 31077 Toulouse Cedex, France, and Laboratoire de Cristallographie, Université de Genève, 30 Quai E. Ansermet, CH 1211 Genève 4, Switzerland

Molecular Crystal Structure and Magnetic Properties of (Croconato)- and (Oxalato)manganese(II) Complexes

Diane Deguenon,[1a] Gérald Bernardinelli,[1b] Jean-Pierre Tuchagues,[1a] and Paule Castan*,[1a]

Received November 21, 1989

The synthesis and IR and magnetic data of four manganese(II) complexes obtained from croconic acid (or potassium croconate) and bipyridyl or imidazole as ligand are described. $[Mn(C_3H_4N_2)_2(C_5O_5)(H_2O)_2]$ (**2**) is built from monomeric units. The compound crystallizes in the triclinic system, space group $P\bar{1}$, with $Z = 2$, $a = 7.405$ (1) Å, $b = 8.672$ (1) Å, $c = 12.139$ (2) Å, $\alpha = 84.84$ (1)°, $\beta = 78.04$ (1)°, $\gamma = 85.53$ (1)°. The structure was solved by direct methods and refined to conventional agreement indices $R = 0.047$ and $R_w = 0.034$ with 1791 observed reflections ($|F_o| > 4\sigma(F_o)$). An extended network of intermolecular hydrogen bonds affords a molecular packing resulting in layers almost perpendicular to the a axis. The interactions between adjacent layers result also from hydrogen bonds. $[Mn(C_{10}H_8N_2)(C_2O_4)]$ (**4**) crystallizes in the orthorhombic system, space group $Pna2_1$, with $Z = 4$, $a = 9.6475$ (6) Å, $b = 9.2578$ (6) Å, and $c = 13.8697$ (9) Å. The structure was solved by direct methods and refined to conventional agreement indices $R = 0.053$ and $R_w = 0.048$ with 1383 observed reflections ($|F_o| > 4\sigma(F_o)$). The crystal is built from infinite chains of oxalato-bridged manganese(II) affording a zigzag structure, the interchain cohesion being established by stacking between the bipyridyl ligands. The magnetic behavior of $[Mn(C_5O_5)(H_2O)_3]$ (**1**) is best described by using a Heisenberg type chain model with interchain interactions. The magnetic data of $[Mn(C_3H_4N_2)_2(C_5O_5)(H_2O)_2]$ (**2**) are best explained by a monomeric structure; however the broadness of the EPR spectra indicates the presence of weak extended intermolecular magnetic interactions, in agreement with the observation of an extended network of intermeolecular hydrogen bonds. From magnetic susceptibility and EPR results obtained for $[Mn(C_{10}H_8N_2)(C_5O_5)\cdot H_2O]$ (**3**), a polymeric structure involving an extended network of hydrogen bonds is assumed. The analysis of the magnetic susceptibility data of **4** indicates that this polymeric complex is a one-dimensional Heisenberg antiferromagnetic chain.

Introduction

Magnetic interactions between paramagnetic metal ions in exchange-coupled systems and magneto–structural correlations in the corresponding transition-metal complexes arouse interest in the inorganic chemistry community. The combination of spin dimensionality, spin quantum number, and the effectiveness of polyatomic bridging ligands in propagating magnetic exchange interactions between transition-metal ions offers a wide range of situations.

During the past decade, several authors[2] have described oxalato-bridged complexes exhibiting large antiferromagnetic exchange interactions. Keeping in mind analogies between oxalate and other oxocarbon ions ($C_4O_4^{2-}$, $C_5O_5^{2-}$), we have investigated some manganese complexes including the croconate dianion sketched in Figure 1.

The croconate dianion, $(C_5O_5)^{2-}$, a member of the cyclic $(CO)_n$ aromatic series that is stabilized by electron delocalization of π electrons all over the ring, has received considerable attention from both theoretical and experimental points of view.[3] However, its coordination chemistry has not been intensively investigated.

In this paper, we report the synthesis, characterization, and IR and magnetic properties of four manganese(II) complexes of croconic or oxalic acid, $[Mn(C_5O_5)(H_2O)_3]$ (**1**), $[Mn(C_5O_5)(imidazole)_2(H_2O)_2]$ (**2**), $Mn(C_5O_5)(bipyridyl)\cdot H_2O$ (**3**), and $[Mn(C_2O_4)(bipyridyl)]$ (**4**), and the molecular and crystal structures of **2** and **4**.

Experimental Section

Materials. Imidazole (ImH) and 2,2′-bipyridyl (bpy) were purchased from Aldrich, and $MnCl_2\cdot 4H_2O$ was purchased from Fluka. Croconic acid and its potassium salt were prepared according to the procedure described by Fatiadi et al.[4]

Complex 1, $[Mn(C_5O_5)(H_2O)_3]$. This compound was prepared as already described.[5] Anal. Calcd for $C_5H_6O_8Mn$: C, 24.11; H, 2.43; Mn, 22.06. Found: C, 23.93; H, 2.41; Mn, 21.93.

Complex 2, $[Mn(C_5O_5)(imidazole)_2(H_2O)_2]$. A water solution (10 mL) of 131 mg (0.66 mmol) of $MnCl_2\cdot 4H_2O$ was slowly added to a water solution of 91 mg (1.34 mmol) of imidazole. To the resultant solution was added an aqueous solution of potassium croconate (0.67 mmol in 5 mL). Shortly thereafter, a fine precipitate formed. The resulting solution was filtered through a fine-porosity frit. About 1 week later, yellow-green needles formed and were isolated, washed with water and ethanol, and dried under vacuum. Anal. Calcd for $C_{11}H_{12}N_4O_7Mn$: C, 35.98; H, 3.29; H, 15.26; Mn, 14.96. Found: C, 35.61; H, 3.24; N, 15.21; Mn, 14.66.

Complex 3, $Mn(C_5O_5)(bipyridyl)\cdot H_2O$. A solution of 116.3 mg (0.74 mmol) of bipyridyl dissolved in 10 mL of ethanol was slowly added to an ethanolic solution of $MnCl_2\cdot 4H_2O$ (147.2 mg in 10 mL). The mixture was stirred for ca. 0.5 h and an aqueous solution of potassium croconate (82 mg in 5 mL) was added, affording a green solution. Transparent yellow-green needles were obtained a few minutes later. Anal. Calcd for $C_{15}H_{10}N_2O_6Mn$: C, 48.79; H, 2.73; H, 7.59; Mn, 14.89. Found: C, 48.78; H, 2.46; N, 7.57; Mn, 14.63.

Complex 4, $[Mn(C_2O_4)(bipyridyl)]$. Croconic acid (63.3 mg in 5 mL of water) and bipyridyl (101.8 mg in 5 mL of ethanol) were mixed together and added to a water solution of $MnCl_2\cdot 4H_2O$ (85.4 mg in 10 mL). Five days later, yellow-green crystals were obtained. In view of their chemical analysis and IR data, they were identified as $[Mn(C_5O_5)(H_2O)_3]$ (**1**). One month later, further evaporation yielded another crop of yellow crystals different from the first ones. The later crystals have been identified as complex **4**. Anal. Calcd for $C_{12}H_8N_2O_4Mn$: C, 48.18; H, 2.69; N, 9.36; Mn, 18.37. Found: C, 48.09; H, 2.63; N, 9.31; Mn, 18.21. Attempts to prepare **4** through direct reaction of either oxalic acid or potassium oxalate with bipyridyl and manganese(II) chloride in a solvent mixture of water and ethanol afforded powder samples of either manganese(II) oxalate hydrate when the water ratio was high or (bipyridyl)manganese(II) oxalate hydrate when the water ratio was low in the solvent mixture.

Physical Measurements. Elemental analyses were carried out at the microanalytical laboratory of the Laboratoire de Chimie de Coordination in Toulouse for C, H and N and at the Service Central de Microanalyse du CNRS in Vernaison for Mn.

IR spectra were recorded on a Perkin-Elmer 983 spectrophotometer coupled with a Perkin-Elmer infrared data station. Samples were run as Nujol mulls.

Variable-temperature magnetic susceptibility data were obtained as previously described[6] on polycrystalline samples with a Faraday-type

† UP 8241 liée par conventions à l'Université Paul Sabatier et à l'Institut National Polytechnique de Toulouse.

(1) (a) Laboratoire de Chimie de Coordination du CNRS. (b) Université de Genève.
(2) (a) Duggan, D. M.; Barefield, E. K.; Hendrickson, D. N. *Inorg. Chem.* **1973**, *12*, 985-991. (b) Jeter, D. Y.; Hatfield, W. E. *Inorg. Chim. Acta* **1972**, *6*, 523-525. (c) Gleizes, A.; Maury, F.; Galy, J. *Inorg. Chem.* **1980**, *19*, 2074-2078. (d) Verdaguer, M.; Julve, M.; Michalowicz, M.; Kahn, O. *Inorg. Chem.* **1983**, *22*, 2624-2629.
(3) (a) Baenziger, N. C.; Hegenbarth, J. J. *J. Am. Chem. Soc.* **1964**, *86*, 3250-3255. (b) Staedli, W.; Hollenstein, R.; von Phillipsborn, W. *Helv. Chim. Acta* **1977**, *60*, 948-958. (c) Flygare, W. H.; Benson, R. C. *J. Mol. Phys.* **1970**, *20*, 225-232.
(4) Fatiadi, A. J.; Isbell, H. S.; Sager, W. F. *J. Res. Natl. Bur. Stand.* **1963**, *67A*, 153-162.
(5) Glick, M. D.; Dahl, L. F. *Inorg. Chem.* **1966**, *5*, 289-293.

0020-1669/90/1329-3031$02.50/0

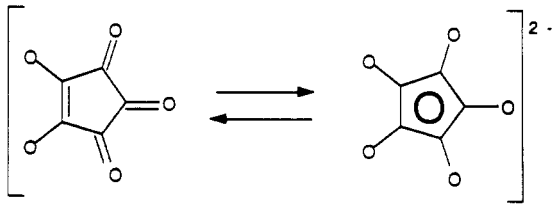

Figure 1. Schematic representation of the croconate dianion, $(C_5O_5)^{2-}$.

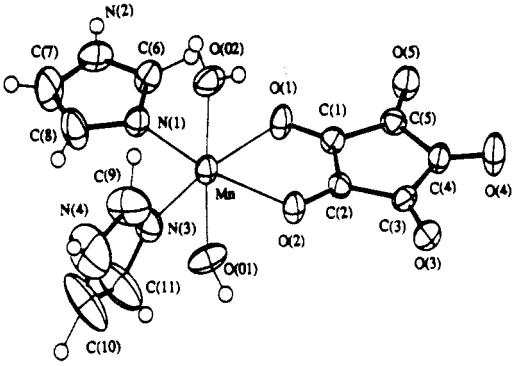

Figure 2. ORTEP view of the $[Mn(C_3H_4N_2)_2(C_5O_5)(H_2O)_2]$ (**2**) molecule.

Table I. Crystallographic Data for **2** and **4**

	2	**4**
formula of the asymmetric unit	$MnC_{11}H_{12}N_4O_7$	$MnC_{12}H_8N_2O_4$
fw	367.2	299.1
a, Å	7.405 (1)	9.6475 (6)
b, Å	8.672 (1)	9.2578 (6)
c, Å	12.139 (2)	13.8697 (9)
α, deg	84.84 (1)	
β, deg	78.04 (1)	
γ, deg	85.53 (1)	
V, Å^3	758.1 (2)	1238.8 (1)
space group	$P\bar{1}$	$Pna2_1$
Z	2	4
d_{obsd}, g·cm^{-3} (flotation)	1.63 (2)	1.59 (2)
d_{calcd}, g·cm^{-3}	1.61	1.60
temp, K	293	293
radiation	Mo Kα (λ = 0.71069 Å, graphite monochromator)	
μ(Mo Kα), cm^{-1}	8.75	10.32
$R = \sum(\|F_o\| - \|F_c\|)/\sum\|F_o\|$	0.047	0.053
$R_w = [(\sum w\|F_o\| - \|F_c\|)^2/\sum w\|F_o\|^2]^{1/2}$	0.034	0.048

magnetometer equipped with a continuous-flow Oxford Instruments cryostat.

Least-squares computer fittings of the magnetic susceptibility data were carried out with an adapted version of the function-minimization program, STEPT.[7]

EPR spectra were obtained on a Bruker 200 TT spectrometer equipped as previously described.[8]

X-ray Crystal Structure Determination of 2 and 4. Pertinent data about the crystals used and the measurement of diffraction intensities are summarized in Table I. Intensities for complex **2** were measured at room temperature on a Philips PW1100 diffractometer; those for compound **4**, on a Nonius CAD-4 diffractometer with graphite-monochromated Mo Kα radiation. Data were corrected for Lorentz and polarization effects but not for absorption since the low value of μr (0.149 and 0.206 for **2** and **4**, respectively) shows that it is not necessary. Atomic scattering factors and anomalous dispersion terms were taken from ref 9. The structures were solved by direct methods (Multan 87)[10] and refined by

(6) Luneau, D.; Savariault, J.-M.; Cassoux, P.; Tuchagues, J.-P. *J. Chem. Soc., Dalton Trans.* **1988**, 1225–1235.
(7) Chandler, J. P. Quantum Chemistry Program Exchange, Indiana University; Program 66.
(8) Mabad, B.; Cassoux, P.; Tuchagues, J.-P.; Hendrickson, D. N. *Inorg. Chem.* **1986**, *25*, 1420–1431.
(9) *International Tables for X-ray Crystallography*; Kynoch Press: Birmingham, U.K., 1974; Vol. IV.

Table II. Non-Hydrogen Atom Positional Parameters for $[Mn(C_3H_4N_2)_2(C_5O_5)(H_2O)_2]$ (**2**) with Estimated Standard Deviations in Parentheses

atom	x	y	z
Mn	0.2452 (1)	0.13282 (9)	0.17811 (6)
O(01)	0.5447 (5)	0.1349 (4)	0.1262 (3)
O(02)	−0.0557 (5)	0.1411 (4)	0.2273 (4)
O(1)	0.2345 (4)	0.0883 (3)	−0.0050 (2)
O(2)	0.2331 (4)	0.3700 (3)	0.0904 (3)
O(3)	0.2210 (4)	0.6293 (3)	−0.0865 (3)
O(4)	0.1874 (5)	0.4895 (4)	−0.2929 (3)
O(5)	0.1984 (5)	0.1523 (4)	−0.2468 (3)
N(1)	0.2641 (5)	−0.1174 (4)	0.2185 (3)
N(2)	0.2601 (6)	−0.3654 (5)	0.2019 (4)
N(3)	0.2652 (6)	0.2163 (5)	0.3391 (3)
N(4)	0.200 (1)	0.2867 (8)	0.5106 (4)
C(1)	0.2240 (6)	0.2174 (5)	−0.0605 (4)
C(2)	0.2268 (6)	0.3621 (5)	−0.0128 (4)
C(3)	0.2192 (6)	0.4878 (5)	−0.0984 (4)
C(4)	0.2034 (7)	0.4192 (5)	−0.2028 (4)
C(5)	0.2085 (6)	0.2482 (5)	−0.1785 (4)
C(6)	0.2435 (7)	−0.2225 (6)	0.1517 (4)
C(7)	0.290 (1)	−0.3496 (6)	0.3049 (6)
C(8)	0.2926 (9)	−0.1977 (6)	0.3154 (5)
C(9)	0.134 (1)	0.2549 (8)	0.4217 (6)
C(10)	0.377 (1)	0.2756 (9)	0.4851 (6)
C(11)	0.421 (1)	0.2269 (9)	0.3806 (5)

Table III. Non-Hydrogen Atom Positional Parameters for $[Mn(C_{10}H_8N_2)(C_2O_4)]$ (**4**) with Estimated Standard Deviations in Parentheses

atom	x	y	z
Mn	0.11606 (9)	0.4060 (1)	0.5000 (0)
N(1)	0.1996 (7)	0.5945 (8)	0.5854 (5)
N(2)	0.0482 (7)	0.6081 (7)	0.4247 (5)
C(1)	0.1689 (9)	0.7270 (9)	0.5548 (6)
C(2)	0.218 (1)	0.848 (1)	0.6026 (9)
C(3)	0.303 (1)	0.832 (1)	0.6797 (9)
C(4)	0.333 (1)	0.697 (1)	0.7122 (7)
C(5)	0.279 (1)	0.584 (1)	0.6628 (7)
C(6)	0.0820 (9)	0.7353 (8)	0.4662 (6)
C(7)	0.036 (1)	0.864 (1)	0.4254 (8)
C(8)	−0.044 (1)	0.861 (1)	0.3422 (8)
C(9)	−0.072 (1)	0.736 (1)	0.3005 (9)
C(10)	−0.029 (1)	0.609 (1)	0.3446 (7)
O(1)	0.4324 (5)	0.1283 (6)	0.5870 (4)
O(2)	0.2315 (5)	0.2475 (6)	0.5863 (5)
O(3)	0.2950 (6)	0.3621 (6)	0.4140 (4)
O(4)	0.4916 (6)	0.2353 (7)	0.4118 (5)
C(01)	0.3450 (8)	0.2118 (8)	0.5512 (5)
C(02)	0.3794 (7)	0.2756 (8)	0.4502 (6)

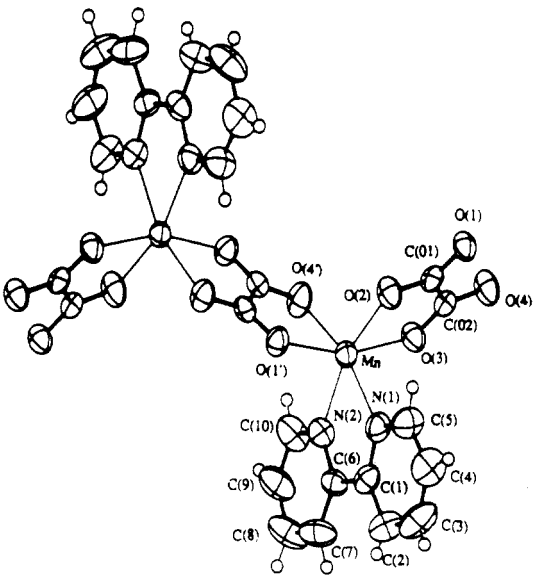

Figure 3. ORTEP view of the $[Mn(C_{10}H_8N_2)(C_2O_4)]$ (**4**) molecule.

Table IV. Selected Interatomic Distances (Å) and Bond Angles (deg) for $[Mn(C_3H_4N_2)_2(C_5O_5)(H_2O)_2]$ (**2**) with Estimated Standard Deviations in Parentheses

Manganese Environment			
Mn-O(01)	2.177 (4)	Mn-O(02)	2.181 (4)
Mn-O(1)	2.309 (3)	Mn-O(2)	2.234 (3)
Mn-N(1)	2.182 (4)	Mn-N(2)	2.181 (5)
O(01)-Mn-O(02)	177.5 (1)	O(01)-Mn-O(1)	88.2 (1)
O(01)-Mn-O(2)	86.8 (1)	O(01)-Mn-N(1)	91.0 (1)
O(01)-Mn-N(3)	89.1 (2)	O(02)-Mn-O(1)	91.5 (1)
O(02)-Mn-O(2)	90.7 (1)	O(02)-Mn-N(1)	91.4 (1)
O(02)-Mn-N(3)	90.8 (2)	O(1)-Mn-O(2)	75.9 (1)
O(1)-Mn-N(1)	89.0 (1)	O(1)-Mn-N(3)	170.0 (1)
O(2)-Mn-N(1)	164.8 (1)	O(2)-Mn-N(3)	94.3 (1)
N(1)-Mn-N(3)	100.7 (2)		
Croconate Ligand			
O(1)-C(1)	1.259 (5)	O(2)-C(2)	1.272 (6)
O(3)-C(3)	1.249 (6)	O(4)-C(4)	1.227 (6)
O(5)-C(5)	1.242 (6)	C(1)-C(2)	1.432 (7)
C(1)-C(5)	1.459 (7)	C(2)-C(3)	1.442 (6)
C(3)-C(4)	1.478 (7)	C(4)-C(5)	1.485 (6)
Mn-O(1)-C(1)	108.3 (3)	Mn-O(2)-C(2)	110.6 (3)
O(1)-C(1)-C(5)	128.4 (4)	C(2)-C(1)-C(5)	108.8 (4)
O(2)-C(2)-C(1)	122.3 (4)	O(2)-C(2)-C(3)	128.2 (4)
C(1)-C(2)-C(3)	109.5 (4)	O(3)-C(3)-C(2)	126.8 (4)
O(3)-C(3)-C(4)	125.8 (4)	C(2)-C(3)-C(4)	107.4 (4)
O(4)-C(4)-C(3)	126.7 (4)	O(4)-C(4)-C(5)	126.0 (5)
C(3)-C(4)-C(5)	107.3 (4)	O(5)-C(5)-C(1)	127.7 (4)
O(5)-C(5)-C(4)	125.4 (4)	C(1)-C(5)-C(4)	106.9 (4)
O(1)-C(1)-C(2)	122.8 (4)		
Imidazole Ligands			
N(1)-C(6)	1.310 (7)	N(1)-C(8)	1.358 (7)
N(2)-C(6)	1.340 (7)	N(2)-C(7)	1.335 (9)
N(3)-C(9)	1.293 (7)	N(3)-C(11)	1.364 (9)
N(4)-C(9)	1.33 (1)	N(4)-C(10)	1.28 (1)
C(7)-C(8)	1.337 (8)	C(10)-C(11)	1.34 (1)
Mn-N(1)-C(6)	125.3 (3)	Mn-N(1)-C(8)	129.1 (4)
C(6)-N(1)-C(8)	105.6 (4)	C(6)-N(2)-C(7)	107.2 (5)
C(9)-N(3)-C(11)	103.2 (5)	C(9)-N(4)-C(10)	108.9 (6)
N(1)-C(6)-N(2)	110.8 (5)	N(2)-C(7)-C(8)	107.1 (5)
N(1)-C(8)-C(7)	109.4 (6)	N(3)-C(9)-N(4)	111.4 (7)
N(4)-C(10)-C(11)	106.0 (8)	N(3)-C(11)-C(10)	110.4 (6)

full-matrix least-squares analysis using the XTAL-2.4 program.[11] All hydrogen atoms have been observed and refined with a fixed value of the isotropic displacement parameters. The final full-matrix least-squares refinement, minimizing $\sum[w(F_o - F_c)^2]$ converged to $R = \sum(|F_o| - |F_c|)/\sum|F_o| = 0.047$ for **2** and 0.053 for **4** and to $R_w = [(\sum w|F_o| - |F_c|)^2/\sum w|F_o|^2]^{1/2} = 0.034$ for **2** and 0.048 for **4** with a weighting scheme $w = 1/\sigma^2(F)$. The goodness of fit was $S = 2.33$ for **2** and 1.13 for **4**. Final fractional atomic coordinates with their estimated standard deviations are gathered in Tables II and III for complexes **2** and **4**, respectively. The ORTEP plots of the molecules are shown in Figure 2 (complex **2**) and Figure 3 (complex **4**) along with the labeling scheme. Selected interatomic distances and angles are listed in Tables IV and V for complexes **2** and **4**, respectively. Complete crystal data and experimental details, components of the anisotropic temperature factors, hydrogen atom positional parameters, deviations of atoms from their least-squares planes, dihedral angles between these planes, and observed and calculated structure factor amplitudes are deposited as supplementary material.

Results and Discussion

Analytical Results and IR Spectroscopy. While the syntheses of **1–3** deserve no special comment, the synthesis of **4** brings up a number of questions. Actually, the analytical and structural data indicate the presence of oxalate anions in complex **4**, while the croconate anions expected to arise from the croconic acid reactant are not identified. This observation indicates that oxidation of the croconic acid occurs during the synthesis with breaking of the croconic cycle and subsequent production of oxalate ions.

Table V. Selected Interatomic Distances (Å) and Bond Angles (deg) for $[Mn(C_{10}H_8N_2)(C_2O_4)]$ (**4**) with Estimated Standard Deviations in Parentheses

Manganese Environment			
Mn-N(1)	2.258 (7)	Mn-N(2)	2.241 (7)
Mn-O(2)	2.197 (6)	Mn-O(3)	2.138 (6)
Mn-O(1′)	2.167 (5)	Mn-O(4′)	2.156 (6)
N(1)-Mn-N(2)	72.7 (3)	N(1)-Mn-O(2)	92.8 (2)
N(1)-Mn-O(3)	98.7 (2)	N(1)-Mn-O(1′)	96.5 (2)
N(1)-Mn-O(4′)	164.9 (2)	N(2)-Mn-O(2)	163.7 (2)
N(2)-Mn-O(3)	97.8 (2)	N(2)-Mn-O(1′)	98.2 (2)
N(2)-Mn-O(4′)	94.5 (2)	O(2)-Mn-O(3)	76.5 (2)
O(2)-Mn-O(1′)	90.8 (2)	O(2)-Mn-O(4′)	100.7 (2)
O(3)-Mn-O(1′)	160.6 (2)	O(3)-Mn-O(4′)	91.0 (2)
O(1′)-Mn-O(4′)	76.8 (2)		

Bipyridyl Ligand					
N(1)-C(1)	1.33 (1)	N(1)-C(5)	1.32 (1)	N(2)-C(6)	1.35 (1)
N(2)-C(10)	1.34 (1)	C(1)-C(2)	1.38 (1)	C(1)-C(6)	1.49 (1)
C(2)-C(3)	1.36 (2)	C(3)-C(4)	1.37 (2)	C(4)-C(5)	1.36 (2)
C(6)-C(7)	1.39 (1)	C(7)-C(8)	1.39 (2)	C(8)-C(9)	1.32 (2)
C(9)-C(10)	1.40 (2)				
C(1)-N(1)-C(5)	117.2 (8)	C(6)-N(2)-C(10)	119.1 (8)		
N(1)-C(1)-C(2)	121.1 (9)	N(1)-C(1)-C(6)	115.8 (7)		
C(2)-C(1)-C(6)	123.1 (8)	C(1)-C(2)-C(3)	120 (1)		
C(2)-C(3)-C(4)	119 (1)	C(3)-C(4)-C(5)	117 (1)		
N(1)-C(5)-C(4)	125 (1)	N(2)-C(6)-C(1)	116.3 (7)		
N(2)-C(6)-C(7)	119.7 (8)	C(1)-C(6)-C(7)	124.0 (8)		
C(6)-C(7)-C(8)	120.0 (9)	C(7)-C(8)-C(9)	120 (1)		
C(8)-C(9)-C(10)	119 (1)	N(2)-C(10)-C(9)	122 (1)		

Oxalato Ligand					
O(1)-C(01)	1.247 (9)	O(2)-C(01)	1.243 (9)	O(3)-C(02)	1.247 (9)
O(4)-C(02)	1.262 (9)	C(01)-C(02)	1.56 (1)		
O(1)-C(01)-O(2)	127.2 (7)	O(1)-C(01)-C(02)	116.7 (6)		
O(2)-C(01)-C(02)	116.1 (6)	O(3)-C(02)-O(4)	125.5 (7)		
O(3)-C(02)-C(01)	117.8 (6)	O(4)-C(02)-C(01)	116.7 (7)		

It is well-known that oxidation of croconic acid leads to leuconic acid.[4,12] Moreover, oxidation of croconic acid by Mo(VI) has been extensively studied by Verchere et al.[13] It proceeds by an outer-sphere mechanism, and an intermediate complex is formed. The final oxidation products are the oxalic and mesoxalic acids.

This type of mechanism, viz. oxidation by a metallic ion, cannot be considered here, since we have shown that this oxidation proceeds in the absence of metal and is photochemically induced. However, this photooxidation yields oxalic and mesoxalic acids as evidenced by UV–vis and ^{13}C NMR spectroscopy.[14]

The infrared spectra of complexes **1–3** display a broad and intense absorption located in the 3400–3000-cm^{-1} range and attributed to the OH stretching frequency of the water molecules while the ν_{HOH} bending affords a strong absorption at 1630 cm^{-1}. In accordance with the West et al. analysis[15] the absorptions observed at 1724, 1719, and 1720 cm^{-1} for compounds **1–3**, respectively, are attributed to the noncoordinated carbonyls of the croconate entity, which exhibits a strong double-bond character, as evidenced by the structural determination. The coordinated C–O groups are characterized by medium absorptions at 1675, 1661, 1676, and 1670 cm^{-1} for **1–4**, respectively. **1–3** exhibit a very strong and broad absorption spanning the range 1650–1350 cm^{-1}, which is characteristic of the salts of $C_nO_n^{2-}$ ion.[16] This absorption may be assigned to vibrational modes representing mixtures of C–O and C–C stretching motions. In **4**, this band is displaced from 1640 to 1500 cm^{-1}. In the far-IR region of the spectra, all four complexes exhibit several absorptions between 430 and 390 cm^{-1}, which may be attributed to the ν_{M-O}(ligand)

(10) Main, P.; Fiske, S. J.; Hull, S. E.; Lessinger, L.; Germain, G.; Declercq, J.-P.; Woolfson, M. M. A System of Computer Programs for the Automatic Solution of Crystal Structures from X-ray Diffraction Data. Universities of York, England, and Louvain-la-Neuve, Belgium, 1987.
(11) Hall, S. R.; Stewart, J. M. XTAL2.4 User's Manual. Universities of Western Australia and Maryland, 1987.
(12) West, R.; Niu, J. *The Chemistry of the Carbonyl Group*; Wiley-Interscience: New York, 1970.
(13) (a) Verchere, J. F.; Fleury, M. B. *J. Less-Common Met.* **1977**, *54*, 135–148. (b) Verchere, J. F.; Fleury, M. B. *Bull. Soc. Chim. Fr.* **1972**, *7*, 2611–2617. (c) Chen, Q.; Liu, S.; Zubieta, J. *Angew. Chem., Int. Ed. Engl.* **1988**, *27*, 1724–1725.
(14) Deguenon, D.; Castan, P. Unpublished results.
(15) West, R.; Niu, Y. H. *J. Am. Chem. Soc.* **1963**, *85*, 2586–2588.
(16) Ito, M.; West, R. *J. Am. Chem. Soc.* **1963**, *85*, 2580–2584.

and ν_{M-O}(water) stretching frequencies.[17] The same IR pattern being observed for **1–3**, it can be considered that the croconate group and the water molecule are coordinated to manganese(II) in complex **3**. Similarly, it seems that the bipyridyl group is coordinated to the metal ion in **3**, as indicated by the shift of the characteristic absorptions[18] (from 995 and 759 cm^{-1} for the free ligand to 1009 and 764 cm^{-1} for **3** and 1009 and 769 cm^{-1} for **4**). The absorptions observed at 244, 238, and 237 cm^{-1} in **2–4**, respectively, are attributed to the Mn–N stretching frequency, in agreement with the attribution made for $[Mn(bpy)_3]^{2+}$.[19] These results allow some insight into the structure of complex **3**: the bipyridyl ligand and the croconate anion are chelated to the manganese(II) ion, the coordination sphere of which is completed with the oxygen atom of a water molecule. The results of the magnetic studies will allow us to specify the monomeric or polymeric structure of this complex (vide infra).

Molecular Structure of 2. The crystal structure of **2** consists of neutral $[Mn(C_3H_4N_2)_2(C_5O_5)(H_2O)_2]$ units. The hexacoordinated manganese atom ($N_2O_2O_{w2}$ ligand environment) is situated at the center of a plane defined by the N(1) and N(3) nitrogen atoms of the imidazole rings and O(1) and O(2) oxygen atoms of the chelated croconate dianion. The two water molecules are axially coordinated.

The Mn–N(1) and Mn–N(3) bond lengths, 2.182 (4) and 2.181 (4) Å, respectively, are in agreement with those reported for other Mn(II) complexes, including manganese–nitrogen bonds.[20] The Mn–O(1) and Mn–O(2) (croconate) distances are equal to 2.309 (3) and 2.234 (3) Å, respectively, while the average Mn–O distance is 2.19 Å in manganese(II) croconate trihydrate.[5] The Mn–O(01) and Mn–O(02) distances (trans water molecules), 2.177 (4) and 2.181 (4) Å, respectively, are approximately equal to the manganese–nitrogen ones. The resulting manganese(II) coordination octahedron is quite severely distorted due to the fact that the two cis croconate Mn–O bonds are significantly longer than the four other bonds. This rhombic distortion of the coordination octahedron, which results from the bite angle of the bidentate croconate anion, is also clearly apparent in the bond angles around the manganese ion (Table IV). The 75.9 (1)° O(1)–Mn–O(2) angle is not significantly different from the corresponding angle found in manganese croconate.[5]

The croconate ligand is planar, although its symmetry is different from the ideal D_{5h} one and although the carbon–carbon bond lengths suggest a partial localization of the π electrons. The 1.432 (7) Å C(1)–C(2) bond is shorter than the other bonds in the ring, indicating that the croconate ring is better described as a quasi croconic acid structure. This assumption is supported by the "ketonic" bond lengths of the uncoordinated oxygen atoms (average value 1.24 Å) compared to the larger C–O bond lengths of the oxygen atoms coordinated to the manganese (average value 1.27 Å).

The geometry of the imidazole ligand is similar to that earlier reported[21] and therefore will not be further discussed. However, while the imidazole ligand including N(1) and N(2) is almost coplanar with the croconate ligand (dihedral angle between the two mean planes 5.7°), the second imidazole ring plane is practically perpendicular to the first one (84.3°).[22]

Of particular interest in this structure is the presence of an extended network of intermolecular hydrogen bonds enhancing the stability of the crystal. All oxygen atoms of the croconate ion (coordinated or not to the Mn(II) ion) are involved in hydrogen bonds with the water and imidazole molecules. The molecular packing affords layers almost perpendicular to the *a* axis of the unit cell and containing the mean coordination plane of the Mn(II) ion with the croconate ion and imidazole molecules. The interactions between the molecules inside a layer results from a hydrogen-bond network involving the croconate and the imidazole molecules whereas the stacking of the layers involves hydrogen bonds between the water molecules and the croconate ions (Figure 4). The interatomic distances and angles corresponding to these hydrogen bonds are given in the supplementary material.

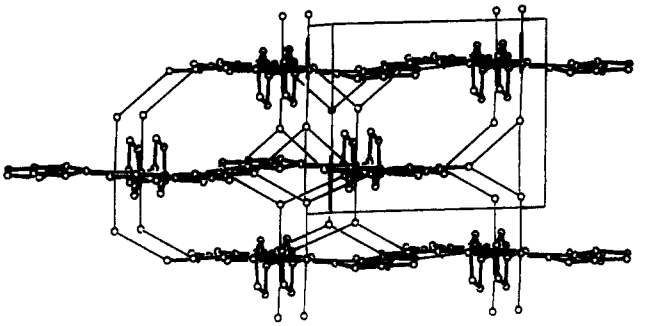

Figure 4. Projection of the unit cell of $[Mn(C_3H_4N_2)_2(C_5O_5)(H_2O)_2]$ (**2**) showing the layers perpendicular to the *a* axis and the hydrogen-bond network between these layers.

Table VI. Summary of Magnetic Susceptibility Data (μ_B/Mn) for Complexes **1–4**

		temp, K				
no.	complex	290	100	50	25	5
1	$[Mn(C_5O_5)(H_2O)_3]$	5.98	5.93	5.79	5.64	4.82
2	$[Mn(C_3H_4N_2)_2(C_5O_5)(H_2O)_2]$	5.95	5.92	5.86	5.73	5.49
3	$Mn(C_5O_5)(C_{10}H_8N_2)\cdot H_2O$	5.96	5.95	5.88	5.77	5.15
4	$[Mn(C_{10}H_8N_2)(C_2O_4)]$	5.68	5.23	4.77	3.95	1.78

Molecular Structure of 4. The structure of **4** consists of neutral $[Mn(bpy)(C_2O_4)]$ units with bridging oxalate anions affording a zigzag chain structure parallel to the *a* axis with an interchain distance of ca. 6.94 Å. The Mn–Mn–Mn angle corresponding to the dihedral angle between two consecutive oxalate mean planes is close to 100° in the present compound.[22] This structure is strongly reminiscent of that of the $[Cu(bpy)(C_2O_4)]\cdot 2H_2O$ complex described by Hathaway et al.[23] The main difference between the two molecular structures results from the presence of uncoordinated water molecules in the copper complex. These water molecules afford short hydrogen-bonding contacts between the infinite chains, whereas there are no such interactions in **4**. The molecular packing of **4** is imposed by an interchain stacking of the bipyridyl ligands (Figure 5a). The bipyridyl groups of two neighboring chains are parallel (the angle between the two mean planes is ca. 2°) but slightly staggered and removed by ca. 4 Å (the shortest contact is N(1)···C(7) = 3.95 Å ($^1/_2 + y$, $^3/_2 - y$, z)). The $N_2O_2O'_2$ ligand environment of the manganese atom is a strongly distorted octahedral structure, resulting from the small bite angle of the three chelating ligands, the bite angle at the bipyridyl ligand is 72.7 (3)°, and those of the two oxalate anions (76.5 (2) and 76.8 (2)°) are not significantly different (Figure 5b).

Although there are no unusual bond lengths and angles in the oxalate and bipyridyl groups, the oxalate ligand is asymmetrically coordinated with a short Mn–O(3) bond (2.138 (6) Å) and a longer Mn–O(2) distance (2.197 (6) Å). This observation is in agreement with the results of the X-ray molecular structure determinations of $[Mn^{II}(C_2O_4)(H_2O)_2]$ (2.22–2.24 Å),[24] $K_2[Mn^{II}(C_2O_4)_2\cdot 2H_2O]$ (2.15–2.25 Å),[25] and $[Mn^{II}_3(C_2O_4)_4(H_2O)_2]^{2-}{}_n$ (2.213–2.152 Å).[26] In all three manganese(II) com-

(17) Nakamoto, K. *Infrared and Raman Spectra of Inorganic and Coordination Compounds*, 4th ed.; Wiley-Interscience: New York, 1982.
(18) McWhinnie, W. R.; Miller, J. D. *Adv. Inorg. Chem. Radiochem.* **1969**, *12*, 135–215.
(19) (a) Saito, Y.; Takemoto, J.; Hutchinson, B.; Nakamoto, K. *Inorg. Chem.* **1972**, *11*, 2003–2011. (b) Takemoto, J.; Hutchinson, B.; Nakamoto, K. *J. Chem. Soc., Chem. Commun.* **1971**, 1007–1011.
(20) Hodgson, D. J.; Schwartz, B. J.; Sorrell, T. N. *Inorg. Chem.* **1989**, *28*, 2226–2228.
(21) Henriksson, H. A. *Acta Crystallogr.* **1977**, *B33*, 1947–1950.
(22) Supplementary material.
(23) Fitzgerald, W.; Foley, J.; McSweeny, D.; Ray, N.; Sheahan, D.; Tyagi, S.; Hathaway, B.; O'Brien, P. *J. Chem. Soc., Dalton Trans.* **1982**, 1117–1121.
(24) Deyrieux, R.; Berro, C.; Pêneloux, A. *Bull. Soc. Chim. Fr.* **1973**, *1*, 25–34.
(25) Schulz, H. *Acta Crystallogr.* **1974**, *B30*, 1318–1332.

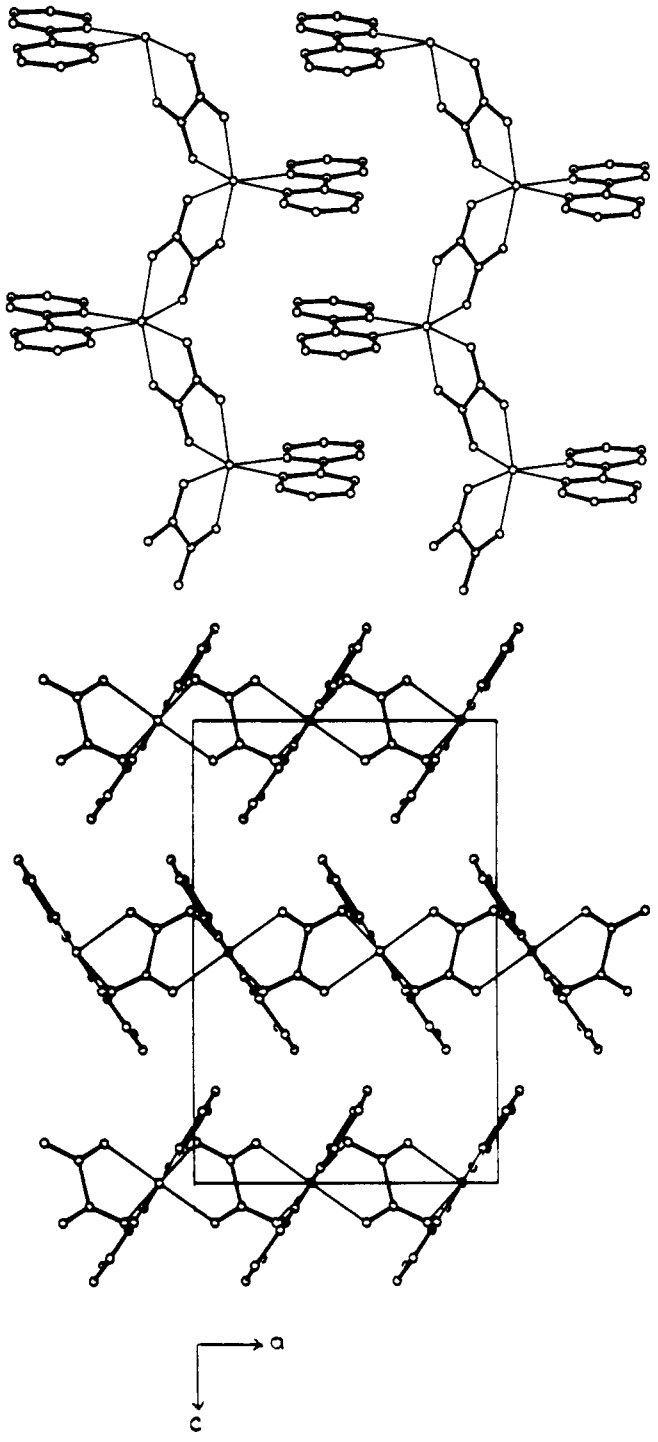

Figure 5. (a) Top: ORTEP view of $[Mn(C_{10}H_8N_2)(C_2O_4)]$ (**4**) showing the interchain stacking of the bipyridyl ligands. (b) Bottom: Projection of **4** onto the *ac* plane.

plexes the metal is chelated to two oxalato ligands, resulting in chain structures. The bipyridyl ligand in **4** is approximately planar, the dihedral angle between the pyridine rings being equal to 4.0 (4)°.

Magnetic Susceptibility and EPR Results. The magnetic susceptibility data for complexes **1**–**4** at 290, 100, 50, 25, and 5 K are listed in Table VI. The detailed data are available as supplementary material. The four complexes studied have effective magnetic moments per manganese(II) ion in the range 5.68–5.98 μ_B at room temperature, indicating the high-spin nature of each complex.

Complex 1. The effective magnetic moment per manganese(II) ion decreases slowly from 5.98 to 5.79 μ_B between 290 and 50 K. The decrease is more pronounced below 50 K, and the magnetic moment reaches 4.82 μ_B at 5 K. The results of the X-ray crystal structure determination of **1** reported by Glick and Dahl[5] indicate a chain structure in which each manganese(II) ion is chelated to one croconate ion and bonded with a single oxygen atom of a second croconate ion. Consequently, two neighboring manganese(II) ions are separated by a croconate ion with a Mn···Mn distance of ca. 7.82 Å inside a chain. Five hydrogen bonds consisting of one intrachain and four interchain CO···H_2O interactions afford a close packing of the chains in a zigzag fashion such that each chain is surrounded by four others displaced by $a/4$, $b/2$ and two are located $a/2$ away. The shortest Mn···Mn interchain distance resulting from this packing is 5.11 Å.

This structural arrangement together with the above-mentioned variation of the magnetic susceptibility and the powder EPR spectra that will be discussed next suggests that spin–spin magnetic interactions are likely to occur between the manganese ions of neighboring chains but are unlikely to occur between the manganese ions inside a chain. The least-squares fitting[22] of the experimental data to the equation for a Heisenberg type chain including interchain interactions[27] affords parameters ($J \approx 0$ cm^{-1}, $\Theta = -3$ K, $g = 1.973$, $R = 5\%$[28]) in agreement with the above-mentioned observations.

The powder X-band EPR spectra of **1** exhibit a temperature-independent and featureless 800 G broad resonance with a 2.029 g value at room temperature. The broadness of this isotropic EPR signal is perfectly consistent with a polymeric manganese(II) structure.[29]

Complex 2. The decrease in the effective magnetic moment of **2** per manganese(II) ion is very weak from 290 to 25 K (5.95–5.73 μ_B) and slightly more pronounced below 25 K (μ_{eff}/Mn = 5.49 μ_B at 5 K).

As described in the molecular structure section, **2** is built from mononuclear $[Mn(C_5O_5)(imidazole)_2(H_2O)_2]$ complex molecules interlinked through a tridimensional hydrogen-bond network involving croconate and water oxygen and imidazole nitrogen atoms. However, the resulting Mn···Mn separations are quite large, the shortest being of 5.650 (1) Å, and involve multiatom bridges unable to transmit exchange magnetic interactions observable through magnetic susceptibility measurements. On the other hand, the distortion of the manganese coordination octahedron is large enough to result in a zero-field splitting of the $^6S_{5/2}$ manganese(II) ground state and afford a small lowering of the magnetic moment below 25 K, as previously observed for several manganese(II) complexes.[8]

The description of the powder X-band EPR spectra of **1** is relevant for **2** except that the spectra are even broader (half-height broadness = 1200 G, $g = 2.022$ at 300 K). As already stated for complex **1**, the broadness of these isotropic signals is consistent with polymeric structures in which spin–spin relaxation is enhanced through large dipolar interactions mediated by the lattice of chains and/or extended hydrogen bonds.[30]

Complex 3. As in the case of **2**, μ_{eff}/Mn decreases slowly from 5.96 to 5.77 μ_B between 290 and 25 K. However, below 25 K,

(26) Wieghardt, K.; Bossek, U.; Nuber, B.; Weiss, J.; Bonvoisin, J.; Corbella, M.; Vitols, S. E.; Girerd, J. J. *J. Am. Chem. Soc.* **1988**, *110*, 7398–7411.

(27) (a) Wagner, G. R.; Friedberg, S. A. *Phys. Lett.* **1964**, *9*, 11–13. (b) Fisher, M. E. *Am. J. Phys.* **1964**, *32*, 343–346. (c) König, E.; Desai, V. P.; Kanellakopoulos, B.; Klenze, R. *Chem. Phys.* **1980**, *54*, 109–113.

(28) The agreement factor R is defined as

$$[\sum_{i=1}^{NP}[\mu_{eff}(obsd)_i - \mu_{eff}(calcd)_i]^2/(NP - k)]^{1/2}$$

where k is the number of variable parameters used to fit the NP data points.

(29) (a) Dowsing, R. D.; Gibson, J. F.; Goodgame, D. M.; Goodgame, M.; Hayward, P. J. *Nature (London)* **1968**, *219*, 1037–1038. (b) Dowsing, R. D.; Gibson, J. F.; Goodgame, M.; Hayward, P. J. *J. Chem. Soc. A* **1969**, 187–193. (c) Dowsing, R. D.; Gibson, J. F.; Goodgame, D. M.; Goodgame, M.; Hayward, P. J. *J. Chem. Soc. A* **1969**, 1242–1248.

(30) (a) Abragam, A.; Bleaney, B. *Résonance Paramagnétique Electronique des Ions de Transition*; Presses Universitaires de France: Paris, 1971. (b) Goodman, B. A.; Raynor, J. B. *Adv. Inorg. Chem. Radiochem.* **1970**, *13*, 205–206.

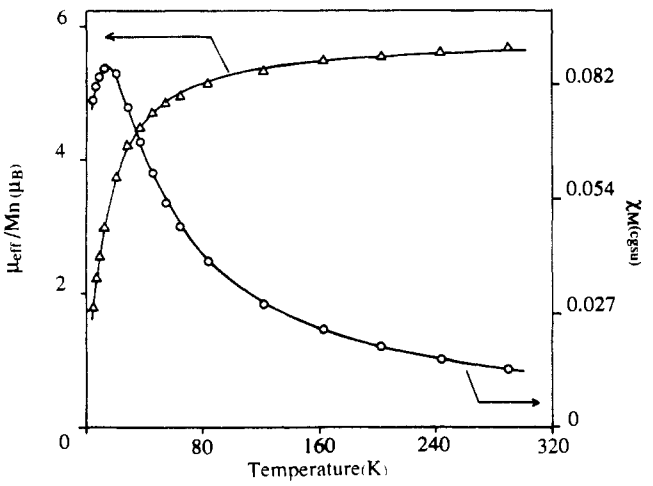

Figure 6. Experimental molar magnetic susceptibility (O) and effective magnetic moment per Mn(II) ion (Δ) vs temperature for **4**. The solid lines represent the least-squares fit of the data to the theoretical equation for isotropic magnetic exchange in a Heisenberg type chain.

the decrease in μ_{eff}/Mn is more pronounced for **3** than for **2** (μ_{eff}/Mn = 5.15 μ_B at 5 K).

The experimental variation of the magnetic susceptibility with temperature has been tentatively analyzed within the framework of two models, affording equally good results: (i) The least-squares fit of the experimental data to the temperature-dependent molar magnetic susceptibility expressed according to the equation for isotropic exchange in a $S_1 = S_2 = 5/2$ dimer[31] modified to take into account interdimer interactions in the molecular field approximation according to the Ginsberg and Lines approach[32] afforded $J = -0.07$ cm^{-1}, $zj' = -0.08$ cm^{-1}, $g_{av} = 2.029$, and paramagnetic impurity = 0% ($R = 2.7\%$). (ii) The least-squares fitting of the experimental data to the equation for a Heisenberg type chain including interchain interactions[27] afforded $J = -0.15$ cm^{-1}, $\Theta = 0.9$ K, and $g_{av} = 2.028$ ($R = 2.5\%$).[22]

With no crystal structure at hand for complex **3**, we relied on IR and EPR spectroscopy to determine the most likely structural hypothesis able to account for the magnetic susceptibility results. The powder X-band EPR spectra of **3** exhibit temperature-independent and featureless broad resonances like those of complexes **1** and **2** (half-height broadness = 2200 G) with a 2.054 g value at 300 K. As stated above for **1** and **2**, the broadness of these isotropic signals is consistent with a polymeric manganese(II) structure, while dimeric structures usually afford EPR signals exhibiting a large number of fine-structure transitions extending over several thousand Gauss.[7] Consequently, the conjunction of the magnetic susceptibility, IR, and EPR results points to a polymeric structure for **3** with a chainlike arrangement of the complex molecules and/or an extended hydrogen-bond network.

Complex 4. The effective magnetic moment per manganese(II) ion is lower than the spin-only value at 290 K (5.68 μ_B) and decreases over the entire temperature range explored, reaching 1.78 μ_B at 5 K. The results of the X-ray crystal structure determination reported in the previous section indicate a chain structure in which the manganese ions are bridged through oxalate dianions and devoid of any interchain hydrogen contacts. Consequently, the magnetic susceptibility data of **4** have been analyzed by using the equation for a Heisenberg type chain.[27] The least-squares fitting of the experimental data affords the solid lines drawn in Figure 6 and the parameters $J = -1.2$ cm^{-1}, $\Theta = -0.04$ K, and $g = 1.967$ ($R = 3\%$). These results indicate that the antiferromagnetic interactions operating in complex **4** involve exclusively intrachain interactions, in agreement with the above-mentioned structural description of this compound, and assess the ideality of the one-dimensional nature of this Heisenberg antiferromagnetic system.

A few examples of characterized chains including exchange-coupled manganese(II) ions have been described, including one-dimensional,[33] two-dimensional,[34] and three-dimensional[35] antiferromagnetic systems. Recently, Unni Nair et al.[36] have described a manganese(II) chain including $[Mn(H_2dapd)Cl_2]$ building units (H_2dapd = 2,6-diacetylpyridine dioxime) and evidenced a small ferromagnetic exchange interaction in this complex (0.2 cm^{-1}). Wieghardt et al.[26] have structurally characterized a $[L_2Mn^{IV}_2(\mu\text{-}O)_2(OH)_2][Mn^{II}_3(C_2O_4)_4(OH_2)_2]\cdot 6H_2O$ complex molecule (L = 1,4,7-triazacyclononane) including polymeric net-shaped anions consisting of interconnected manganese(II)–oxalate chains. They have qualitatively interpreted the variation of the bulk magnetic susceptibility of this complex with temperature by postulating that the Mn(II) centers in the polymeric anion are not exchange-coupled while the Mn(IV) centers in the dimeric cation are strongly antiferromagnetically coupled. In the $[Mn_2L^1(CH_3CO_2)(ClO_4)]_n$ and $[Mn_2L^2(CH_3CO_2)(ClO_4)]_n$ complexes recently described by J.-P.T.,[6] the binuclear units are bridged by acetate anions into infinite chains. The high-spin manganese(II) ions exhibit a weak intramolecular antiferromagnetic exchange interaction ($J = -0.8$ cm^{-1}) in both complexes. The extended intermolecular interactions mediated by the acetato groups between the manganese ions in a chain are very weak and not sensed through the magnetic susceptibility measurements but still reflected by the powder EPR spectra. Surprisingly, the magnetic behavior of manganese(II) oxalate has not been reported although the X-ray crystal structure evidences a chain structure,[24] the magnetic properties of which should be interesting to explore. For comparison purposes, we have prepared this salt and studied the variation of its magnetic susceptibility with temperature in the 300–4 K range. The least-squares fitting of the experimental data using the equation for a Heisenberg type chain affords the parameters $J = -0.9$ cm^{-1}, $\Theta = -0.01$ K, and $g = 2.027$ ($R = 2.9\%$). Consequently, the magnetic behavior of this manganese–oxalate chain is very similar to that of complex **4**, in agreement with their structural similarities.

This survey of the magnetic properties of the manganese(II) chains already described clearly shows that, among the multiatom bridges, the oxalato ones are able to transmit magnetic superexchange interactions between manganese(II) ions similar to those transmitted by the sulfate bridges in the case of $Mn^{II}(N_2H_5)_2(SO_4)_2$.[35] In this compound, the Mn···Mn separation is ca. 5.3 Å and involves O–S–O bridges, while the Mn···Mn separation in **4** is 5.622 (1) Å and involves O–C–O bridges. Finally, among the multiatom bridges already used, the oxalato and sulfato ones are able to mediate measurable magnetic superexchange interactions between manganese(II) ions while the croconato and the acetato ones are not.

The powder X-band EPR spectra of **4** exhibit a temperature-independent and featureless sharp resonance (half-height broadness = 190 G) with a 1.998 g value at 300 K. This unusual EPR behavior has already been reported for a dodecamanganese(II) complex[37] and for systems consisting of n divalent manganese(II) ions coupled together by exchange interactions.[38-42] This behavior

(31) O'Connor, C. J. *Prog. Inorg. Chem.* **1982**, *29*, 203–283.
(32) Ginsberg, A. P.; Lines, M. E. *Inorg. Chem.* **1972**, *11*, 2289–2290.
(33) (a) Caputo, R. E.; Roberts, S.; Willett, R. D.; Gerstein, B. C. *Inorg. Chem.* **1976**, *15*, 820–823. (b) McElearney, J. N. *Inorg. Chem.* **1976**, *15*, 823–827. (c) Caputo, R. E.; Willett, R. D. *Phys. Rev. B* **1976**, *13*, 3956–3960. (d) McElearney, J. N.; Merchant, S.; Carlin, R. L. *Inorg. Chem.* **1973**, *12*, 906–910. (e) Caputo, R. E.; Willett, R. D.; Morosin, B. *J. Chem. Phys.* **1978**, *69*, 4976–4981. (f) Estes, W. E.; Weller, R. R.; Hatfield, W. E. *Inorg. Chem.* **1980**, *19*, 27–32.
(34) (a) Groenendijk, H. A.; van Duyneveldt, A. J.; Willett, R. D. *Physica* **1979**, *98B*, 53–58. (b) Losee, D. B.; McGregor, K. T.; Estes, W. E.; Hatfield, W. E. *Phys. Rev. B* **1976**, *14*, 4100–4105.
(35) Witteveen, H. T.; Reedijk, J. *J. Solid State Chem.* **1974**, *10*, 151–166.
(36) Unni Nair, B. C.; Sheats, J. E.; Ponteciello, R.; Van Engen, D.; Petrouleas, V.; Dismukes, G. C. *Inorg. Chem.* **1989**, *28*, 1582–1587.
(37) Luneau, D.; Savariault, J. M.; Tuchagues, J. P. *Inorg. Chem.* **1988**, *27*, 3912–3918.
(38) Gorter, C. J.; Van Vleck, J. H. *Phys. Rev.* **1947**, *72*, 1128–1129.
(39) Van Vleck, J. H. *Phys. Rev.* **1948**, *74*, 1168–1183.
(40) Van Wieringen, J. S. *Discuss. Faraday Soc.* **1955**, *19*, 118–126.
(41) Matumura, O. *Mem. Fac. Sci., Kyushu Univ.* **1958**, *B2*, 175–179.
(42) Schneider, E. E.; England, T. S. *Physica* **1951**, *17*, 221–233.

has been rationalized for the first time by Kubo and Tomita,[43] who have set up the basis of the theory used to explain the exchange-narrowing phenomenon.[44] When the anisotropic interactions are negligible and the exchange integrals are much larger than the hyperfine constant ($|J_{ij}| \gg |A|$), which is presently the case, the system may be regarded as being approximately in an eigenstate of S^2 and S_z. This leads to the inhomogeneous exchange-narrowing situation described by Ishikawa.[45] The EPR spectra of complex **4** show evidence for the first time of the inhomogeneous exchange-narrowing phenomenon in the powder spectra of an infinite chain of manganese(II) ions antiferromagnetically exchange-coupled through oxalato bridges.

Concluding Remarks

This study points out that croconato bridges are unable to mediate significant spin-spin magnetic exchange interactions between the manganese(II) ions of an infinite chain. In this regard, the behavior of the croconato anion is similar to that of the acetato anion.[6] This study also clearly establishes for the first time that, unlike the croconato dianion or the acetato monoanion, the oxalato dianion is able to mediate small magnetic superexchange interactions between the manganese(II) ions of an infinite chain, of the order of magnitude of those estimated in the case of sulfato bridges.[35] However, at variance with the case of the sulfato-bridged manganese(II) chain, complex **4** and manganese(II) oxalate behave as one-dimensional antiferromagnets.

Supplementary Material Available: Figures 7 and 8, showing the least-squares fit of the experimental molar magnetic susceptibility and effective magnetic moment data per Mn(II) ion to the theoretical equation for isotropic magnetic exchange in a Heisenberg type chain for **1** and **3**, respectively, Tables VII-XIV, listing crystallographic data, hydrogen atom positional parameters, final non-hydrogen atom thermal parameters, deviations of atoms from their least-squares planes, and dihedral angles between these planes for complexes **2** and **4**, respectively, and interatomic distances for the hydrogen-bonded atoms of complex **2**, Tables XVII-XIX, listing the experimental magnetic susceptibility data for complexes **1**, **3**, and **4**, respectively (14 pages); Tables XV and XVI, listing observed and calculated structure factor amplitudes for complexes **2** and **4**, respectively (24 pages). Ordering information is given on any current masthead page.

(43) Kubo, R.; Tomita, K. *J. Phys. Soc. Jpn.* **1954**, *9*, 888-919.
(44) Pake, G. E. In *Paramagnetic Resonance*; Pines, D., Ed.; W. A. Benjamin, Inc.: Reading, MA, 1962; pp 89-95, 140-152.
(45) Ishikawa, Y. *J. Phys. Soc. Jpn.* **1966**, *21*, 1473-1481.

Contribution from the Departments of Chemistry, The Chung-Cheng Institute of Technology, Taiwan, Republic of China, and The University of Mississippi, University, Mississippi 38677

Lower Valence Fluorides of Chromium. 2. The Phase K_xCrF_3 (x = 0.43-0.59)

Y. S. Hong,† K. N. Baker, Jr.,‡ A. V. Shah,‡ R. F. Williamson,‡ and W. O. J. Boo*,‡

Received September 14, 1989

Chemical analyses verify that the composition of K_xCrF_3 ranges from $x = 0.43$ to $x = 0.59$. Three structures were found to coexist within this composition: a $BaTa_2O_6$ type hexagonal structure ($x < 0.50$), a $BaTa_2O_6$ type structure distorted to orthorhombic ($x \approx 0.50$), and a tetragonal tungsten bronze type structure distorted to orthorhombic ($x > 0.50$). From symmetry lowering associated with concomitant ionic ordering, the tetragonal tungsten bronze type structure was deduced to belong to space group C^6_{2v}-$Pba2$.

Introduction

Numerous ternary- and quaternary-phase fluorides of first-row transition metals have been prepared and characterized in this laboratory.[1-6] From careful X-ray diffraction and magnetic measurements on randomly oriented powdered samples, we have concluded that it is the nature of these materials to display various kinds of concomitant ionic ordering at room temperature.

The fluoride systems K_xFeF_3[7] and K_xVF_3[8,9] ($x \approx 0.4$-0.6) were reported to crystallize in the tetragonal tungsten bronze structure. Magnetic measurements made on the vanadium fluoride system support the conclusion that V^{2+} and V^{3+} ions are ordered.[1] This ordering lowers the crystal symmetry from D^5_{4h}-$P4/mbm$ (reported for K_xWO_3[10]) to C^6_{4v}-$P4_2bc$ (reported for $KMnFeF_6$[11]). The K_xCrF_3 system (x = 0.44-0.60), however, was reported by Dumora et al.[12] not to form the tetragonal bronze structure. Instead, a hexagonal structure related to that of $BaTa_2O_6$[13] was formed. Neither variations in the structure of K_xCrF_3 with composition nor evidence of concomitant ionic ordering (such as small crystal distortions or superstructures) was reported; and no mention was made of magnetic measurements. They did, however, report an attempt to prepare single crystals from the melt (850 °C), which produced some monocrystals with hexagonal lattice parameters a = 21.53 Å and c = 7.610 Å.

The reason the tetragonal tungsten bronze structure did not form for K_xCrF_3 was believed to be related to the Jahn-Teller ion, Cr^{2+}, but there may be conditions under which the bronze structure will form. If the tetragonal bronze phase does form, we would expect to observe Jahn-Teller cooperative ordering in addition to ordering of Cr^{2+} and Cr^{3+} ions. This additional order should further lower its crystal symmetry.

We chose to study the K_xCrF_3 phase (x = 0.44-0.60) to determine if ordering phenomena or other composition-dependent properties may exist at room temperature. Our initial characterization (A series) was so surprisingly different from the results of the French authors[12] that we repeated the synthesis (B series).

Experimental Section

Appropriate quantities of KF, CrF_2, and CrF_3 were vacuum-encap-

†The Chung-Cheng Institute of Technology.
‡The University of Mississippi.

(1) Hong, Y. S.; Williamson, R. F.; Boo, W. O. J. *Inorg. Chem.* **1980**, *19*, 229.
(2) Hong, Y. S.; Williamson, R. F.; Boo, W. O. J. *Inorg. Chem.* **1981**, *20*, 403.
(3) Banks, E.; Shone, M.; Hong, Y. S.; Williamson, R. F.; Boo, W. O. J. *Inorg. Chem.* **1982**, *21*, 3894.
(4) Hong, Y. S.; Williamson, R. F.; Boo, W. O. J. *Inorg. Chem.* **1982**, *21*, 3898.
(5) Hong, Y. S.; Baker, K. N.; Williamson, R. F.; Boo, W. O. J. *Inorg. Chem.* **1984**, *23*, 2787.
(6) Williamson, R. F.; Arafat, E. S.; Baker, K. N.; Rhee, C. H.; Sanders, J. R.; Scheffler, T. B.; Zeidan, H. S.; Boo, W. O. J. *Inorg. Chem.* **1985**, *24*, 482.
(7) dePape, R. *Bull. Soc. Chim. Fr.* **1965**, 3489.
(8) Garrard, B. J.; Wanklyn, B. M.; Smith, S. H. *J. Cryst. Growth* **1974**, *22*, 169.
(9) Cros, C.; Feurer, R.; Pouchard, M.; Hagenmuller, P. *Rev. Chim. Miner.* **1974**, *11*, 585.
(10) Magneli, A. *Ark. Kemi* **1949**, *11*, 213.
(11) Banks, E.; Nakajima, S.; Williams, G. J. B. *Acta Crystallogr.* **1979**, *B35*, 46.
(12) Dumora, D.; Raney, J.; Hagenmuller, P. *Bull. Soc. Chim. Fr.* **1970**, *5*, 1751.
(13) Layden, G. K. *Mater. Res. Bull.* **1968**, *3*, 349.

0020-1669/90/1329-3037$02.50/0